

# THE SPECTRAL CONTENT OF A SAGGING STRING

ARYAMAN CHANDRA<sup>1</sup> AND SUDHIR RANJAN JAIN<sup>2</sup>

<sup>1</sup>Heritage Xperiential Learning School  
CRPF Rd, Sector 62  
Gurugram, Haryana 122005

<sup>2</sup>Department of Information Technology  
K. J. Somaiya School of Engineering  
Somaiya Vidyavihar University  
Vidyavihar, Mumbai 400072

**ABSTRACT.** This paper develops a precise correspondence between the static deformation of an interval and the spectral structure of the Dirichlet Laplacian. The torsion function generated by a uniform load decomposes into local quadratic profiles that coincide with the nodal intervals of each eigenfunction, while the reciprocal of each local profile identifies the unique extremum of the corresponding vibrational mode. These local descriptions are unified by a global spectral expansion that expresses the torsion function as a uniformly convergent superposition of all odd eigenfunctions. The results provide a complete one dimensional framework in which equilibrium geometry, nodal structure, and vibrational behaviour are fully aligned.

## 1. INTRODUCTION

In the study of a vibrating medium, one often distinguishes two phenomena. There is the quiet, static shape a membrane assumes under a uniform load, and there are the oscillations it exhibits when struck. The first belongs to equilibrium, the second to sound, and the mathematics assigns them to two equations of very different temperaments: the equilibrium profile solves the Poisson problem, while the vibrational modes solve the eigenvalue problem for the Laplacian.

Kac once asked whether one can hear the shape of a drum—that is, whether the spectrum of the Laplacian suffices to reconstruct the geometry of the domain [1]. The question is charming, yet precise. In this paper, we ask the inverse question in an equally literal sense: can the static shape hear the drum? Does the deformation of an interval under a uniform load contain, hidden within its curvature, the information of all its vibrational modes?

In one dimension, the answer is affirmative. The landscape function, the solution of the Poisson equation with Dirichlet boundary conditions, encodes the nodal structure and amplitude maxima of every eigenfunction of the Dirichlet Laplacian. In this simplest setting, the mechanism that Filoche and Mayboroda identified for disordered media becomes exact [2, 3]: the reciprocal of the landscape pinpoints the amplitude peaks of each mode, and the landscape itself is an infinite superposition of the odd eigenfunctions.

## 2. RELATED WORK AND CONTEXT

The question of connecting geometry to spectrum has a long history. Kac’s famous 1966 paper [1] initiated the study of how the spectrum of the Laplacian encodes geometric information about a domain. While early results established that certain shapes are determined uniquely by their spectrum, counterexamples later revealed that isospectral domains with different geometries exist, highlighting the subtlety of the inverse problem.

More recently, attention has turned to understanding how local geometric features influence spectral properties. Filoche and Mayboroda [2, 3] introduced the *localization landscape* to predict

wave confinement in complex and disordered media. Their work demonstrated that the solution to a simple Poisson problem, when viewed appropriately, encodes where eigenfunctions concentrate, providing both heuristic and computational insight into localization phenomena.

Beyond disordered media, the study of Sturm-Liouville operators and their eigenfunctions has produced a rich body of results characterizing nodal sets [5], eigenvalue distributions, and amplitude extrema [12, 4, 11]. These classical theorems provide rigorous foundations for understanding how boundary conditions and operator structure determine spectral behavior.

Our work bridges these strands. By restricting attention to the one-dimensional Dirichlet Laplacian, we isolate the precise geometric mechanism underlying the landscape function. In doing so, we replace heuristic predictions with exact statements, establishing an explicit correspondence between static deformation and the full spectrum of vibrational modes. This approach complements the broader literature, providing a rigorous foundation in a setting that is simple enough to allow complete analysis, yet rich enough to reveal fundamental principles relevant to higher-dimensional and more complex systems.

### 3. MATHEMATICAL FOUNDATIONS

This section collects the analytic structures that underpin all later arguments. The aim is to formalise the connection between the static Poisson problem, the spectral theory of the Dirichlet Laplacian, and the Green kernel for the interval. Each object is introduced with the level of precision required for the results that follow and no more.

**3.1. The eigenvalue problem on the interval.** Let  $\Omega = (0, 1)$  and consider the Dirichlet Laplacian  $L = -\frac{d^2}{dx^2}$  acting on  $L^2(\Omega)$  with domain  $H^2(\Omega) \cap H_0^1(\Omega)$ . The eigenvalue problem

$$(1) \quad L\psi = \lambda\psi, \quad \psi(0) = \psi(1) = 0,$$

is the standard Sturm-Liouville system on the interval. For  $\lambda > 0$ , the general solution is  $\psi(x) = A \sin(\sqrt{\lambda}x) + B \cos(\sqrt{\lambda}x)$ . The boundary condition at  $x = 0$  forces  $B = 0$ ; the condition at  $x = 1$  implies  $\sin(\sqrt{\lambda}) = 0$ . The spectrum is therefore

$$(2) \quad \lambda_n = (n\pi)^2, \quad n \in \mathbb{N},$$

and the corresponding  $L^2$  normalised eigenfunctions are

$$(3) \quad \psi_n(x) = \sqrt{2} \sin(n\pi x).$$

Classical properties follow from Sturm-Liouville theory. The function  $\psi_n$  has exactly  $n - 1$  interior zeros, which form the nodal set

$$(4) \quad \mathcal{N}_n = \left\{ \frac{k}{n} : k = 1, 2, \dots, n-1 \right\}.$$

These points partition  $\Omega$  into  $n$  equal subintervals

$$(5) \quad \mathcal{I}_{n,j} = \left[ \frac{j}{n}, \frac{j+1}{n} \right], \quad j = 0, 1, \dots, n-1,$$

on each of which the eigenfunction has a single sign. These intervals will serve as the basic geometric units in later spectral estimates.

**3.2. The Poisson problem and the landscape function.** We next consider the static deformation of the string. For a uniform load, the landscape function is the unique solution of

$$(6) \quad -u''(x) = 1, \quad x \in (0, 1), \quad u(0) = u(1) = 0.$$

Integrating twice yields

$$(7) \quad u(x) = \frac{1}{2}x(1 - x).$$

The function  $u$  is smooth on the closed interval, strictly positive on the interior, and strictly concave. It attains its maximum at  $x = \frac{1}{2}$ . These properties follow directly from the maximum principle and from the constant negative second derivative.

The reciprocal landscape

$$(8) \quad W(x) = \frac{1}{u(x)} = \frac{2}{x(1 - x)},$$

is singular at the boundary and convex on every compact subset of the interior. Although defined pointwise, it will later appear in integral inequalities that control eigenfunction amplitudes. The singularities of  $W$  encode the effective confinement created by the vanishing of  $u$  at the boundary.

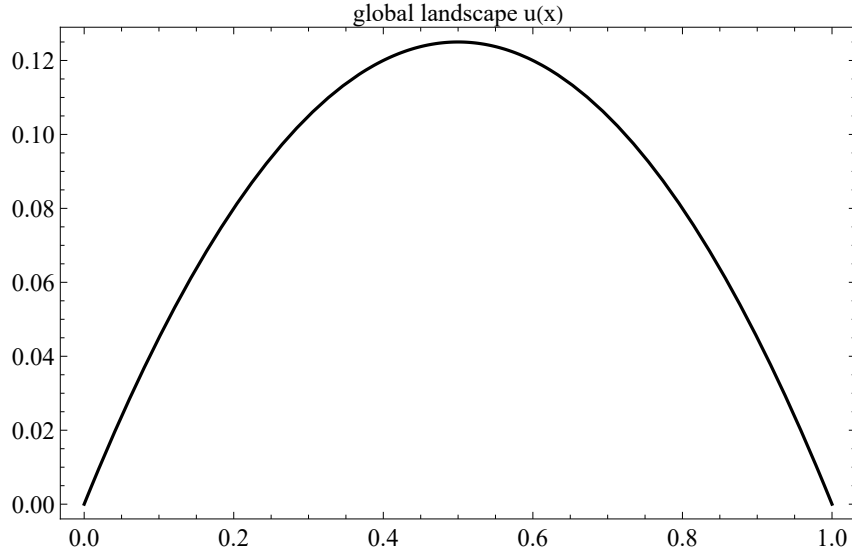


FIGURE 1. Global landscape  $u(x) = \frac{1}{2}x(1 - x)$  on the unit interval. The function is strictly concave and vanishes at the endpoints.

**3.3. The Green function and the spectral expansion.** The analytic link between the static and dynamic problems is the Green function for the Dirichlet Laplacian. It is defined by

$$(9) \quad -LG(x, \xi) = \delta(x - \xi), \quad G(0, \xi) = G(1, \xi) = 0,$$

in the distributional sense. For the interval, the explicit expression is

$$(10) \quad G(x, \xi) = \begin{cases} x(1 - \xi), & 0 \leq x \leq \xi \leq 1, \\ \xi(1 - x), & 0 \leq \xi \leq x \leq 1. \end{cases}$$

The operator  $L^{-1}$  is compact and self adjoint, which yields the Hilbert-Schmidt expansion

$$(11) \quad G(x, \xi) = \sum_{n=1}^{\infty} \frac{\psi_n(x) \psi_n(\xi)}{\lambda_n}.$$

The series converges uniformly on  $[0, 1]^2$  since the kernel is smooth and the coefficients decay like  $n^{-2}$ . This identity is the analytic bridge that will allow us to recover the landscape as a spectral sum in later sections and to interpret  $u$  as a geometric average of eigenfunctions.

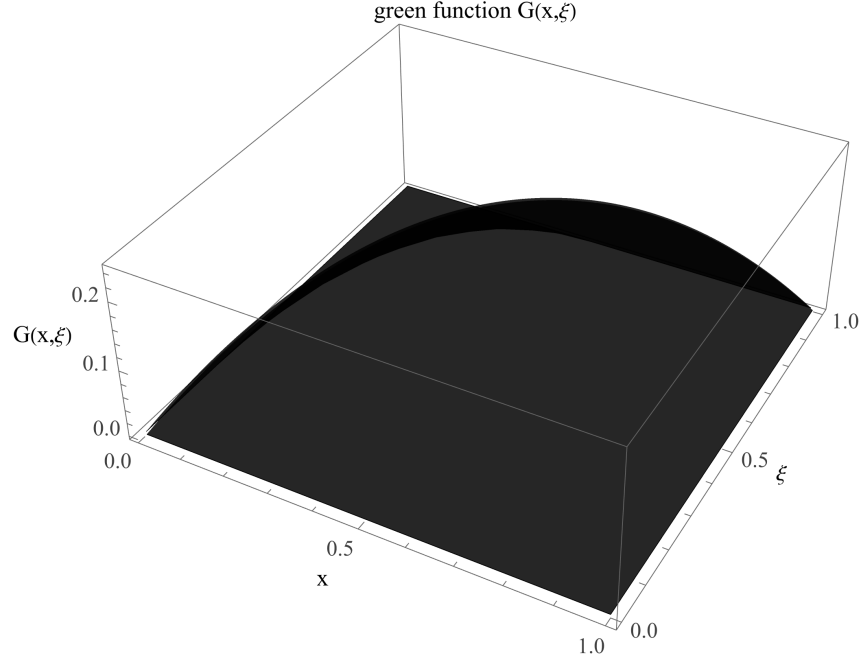


FIGURE 2. Green function  $G(x, \xi)$  for the Dirichlet Laplacian on  $(0, 1)$ . The kernel is symmetric and vanishes on the boundary.

This framework completes the foundations required for the subsequent theorems. Every later estimate draws on the operator structure established above, the explicit geometry of the eigenfunctions, and the representation of the inverse operator through its Green kernel.

**3.4. Notation.** The principal symbols used throughout the paper are listed below.

Symbol	Description
$\Omega$	the unit interval $(0, 1)$
	the one dimensional Laplacian
$u$	the global landscape, defined by $-u'' = 1$ on $\Omega$
$G(x, \xi)$	the Dirichlet Green function on $\Omega$
$\psi_n$	normalized Dirichlet eigenfunctions of
$\lambda_n$	eigenvalues associated with $\psi_n$
$\mathcal{I}_{n,j}$	the $j$ th nodal interval of $\psi_n$
$u_{n,j}$	local landscape on $\mathcal{I}_{n,j}$
$W_{n,j}$	reciprocal landscape $W_{n,j} = 1/u_{n,j}$

## 4. MAIN RESULTS

The preliminaries established the spectral geometry of the Dirichlet Laplacian, the structure of its nodal partitions, and the behaviour of both the global and local landscape functions. We now turn to the central theorems of the paper, which formalize the connections suggested by this structure. Each result isolates a different aspect of the relationship between the static Poisson problem and the dynamic eigenvalue problem. The first describes how the landscape decomposes into a family of local quadratics adapted to the nodal intervals of a single eigenfunction. The second shows that the reciprocal of each local landscape identifies, with complete precision, the location where the corresponding eigenfunction attains its maximal amplitude. The third establishes that the global landscape is the unique spectral superposition of all odd eigenmodes, a representation that is both uniform and rapidly convergent. Together these results form a unified dictionary between static deformation and spectral behaviour, showing that the geometry of the landscape encodes both nodal structure and amplitude localization, and that the landscape itself arises from an exact spectral expansion.

**4.1. The Segmental Landscape Theorem.** The first result shows how the global landscape decomposes into a mosaic of local quadratics, each adapted to the nodal partition of a single eigenfunction.

**Theorem 1** (Segmental Landscape Theorem). *Let  $\mathcal{I}_{n,j} = [j/n, (j+1)/n]$  be the  $j$ th nodal interval of  $\psi_n$ . Then there exists a unique function  $u_{n,j} : \mathcal{I}_{n,j} \rightarrow \mathbb{R}$  satisfying*

$$(12) \quad -u_{n,j}''(x) = 1, \quad x \in \mathcal{I}_{n,j},$$

*together with the boundary conditions*

$$(13) \quad u_{n,j}(j/n) = 0, \quad u_{n,j}((j+1)/n) = 0.$$

*Moreover,  $u_{n,j}$  is the quadratic polynomial*

$$(14) \quad u_{n,j}(x) = \frac{1}{2} \left( x - \frac{j}{n} \right) \left( \frac{j+1}{n} - x \right),$$

*and its zeros coincide exactly with the nodal points of  $\psi_n$  on the interval  $\mathcal{I}_{n,j}$ .*

*Proof.* The differential equation  $-u'' = 1$  integrates to

$$u(x) = -\frac{x^2}{2} + Ax + B$$

for constants  $A$  and  $B$ . Imposing  $u(j/n) = 0$  and  $u((j+1)/n) = 0$  yields two linear equations:

$$(15) \quad -\frac{1}{2} \left( \frac{j}{n} \right)^2 + A \frac{j}{n} + B = 0,$$

$$(16) \quad -\frac{1}{2} \left( \frac{j+1}{n} \right)^2 + A \frac{j+1}{n} + B = 0.$$

Subtracting these equations gives

$$A \cdot \frac{1}{n} = \frac{1}{2n^2} [(j+1)^2 - j^2] = \frac{2j+1}{2n^2},$$

so  $A = (2j+1)/(2n)$ . Substituting back determines  $B = -j(j+1)/(2n^2)$ .

Inserting these constants into the general form and simplifying produces the factorized expression

$$u_{n,j}(x) = \frac{1}{2} \left( x - \frac{j}{n} \right) \left( \frac{j+1}{n} - x \right),$$

which is nonnegative on  $\mathcal{I}_{n,j}$ , concave, symmetric about  $(2j+1)/(2n)$ , and vanishes precisely at the nodal points. Uniqueness follows from the standard theory of second order ODEs with Dirichlet data.  $\square$

*Remark 1.* The function  $u_{n,j}$  is not the restriction of the global landscape  $u(x) = \frac{1}{2}x(1-x)$  to  $\mathcal{I}_{n,j}$ , but rather a mode adapted landscape determined solely by the nodal boundary conditions of  $\psi_n$ . The family  $\{u_{n,j}\}_j$  therefore encodes the eigenfunction's nodal geometry through a purely local and universal forcing. Different eigenfunctions generate different local landscapes, revealing how the same static equation captures mode dependent structure.

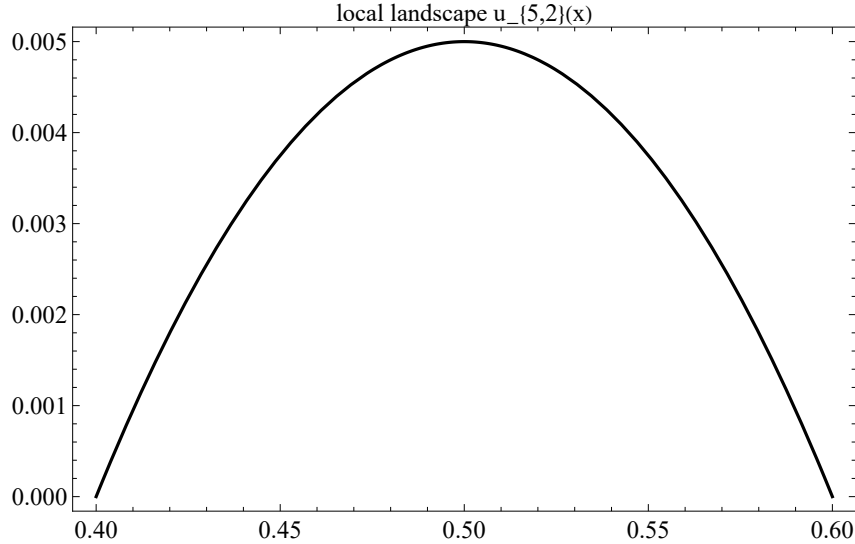


FIGURE 3. Local landscape  $u_{n,j}$  on the interval  $[2/5, 3/5]$  for  $n = 5$ . The function vanishes at the nodal points and attains its unique interior maximum at the midpoint.

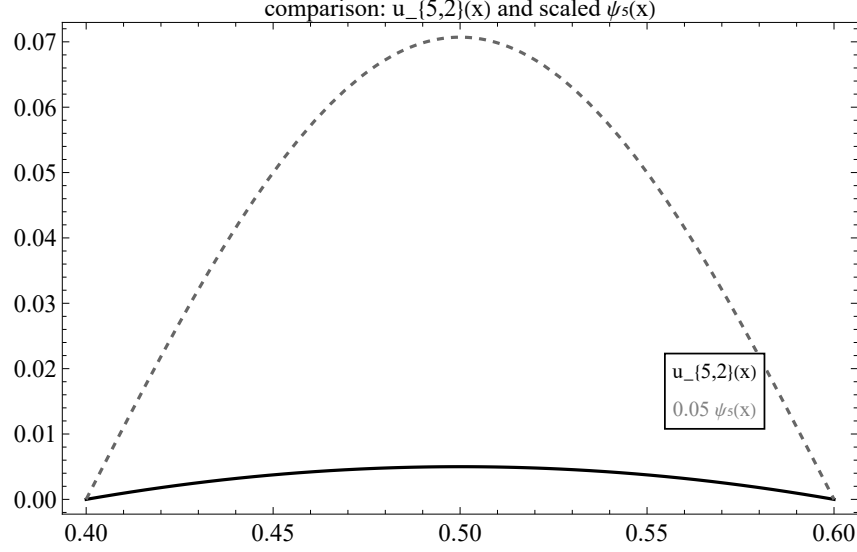


FIGURE 4. Comparison of the local landscape  $u_{n,j}(x)$  and the scaled eigenfunction  $\psi_5(x)$  on  $[2/5, 3/5]$ . Both vanish at the endpoints, demonstrating the exact nodal correspondence established in Theorem 1.

**4.2. The Principle of Reciprocal Localization.** While the landscape determines the nodal partition, its reciprocal identifies the points where the eigenfunction attains its amplitude extrema.

**Theorem 2** (Principle of Reciprocal Localization). *Let  $W_{n,j}(x) = 1/u_{n,j}(x)$  be the reciprocal landscape on the nodal interval  $\mathcal{I}_{n,j} = [j/n, (j+1)/n]$ . Then  $W_{n,j}$  attains its unique minimum at*

$$(17) \quad x_{n,j}^* = \frac{2j+1}{2n},$$

*and this point coincides with the unique extremum of the eigenfunction*

$$\psi_n(x) = \sqrt{2} \sin(n\pi x)$$

*in the same interval.*

*Proof.* The eigenfunction derivative is

$$\psi'_n(x) = \sqrt{2} n\pi \cos(n\pi x),$$

so the critical points of  $\psi_n$  occur where  $\cos(n\pi x) = 0$ , that is,

$$n\pi x = \left(k + \frac{1}{2}\right) \pi.$$

On the interval  $\mathcal{I}_{n,j}$  of length  $1/n$ , exactly one such value lies inside the interval, namely  $x_{n,j}^* = (2j+1)/(2n)$ .

For the reciprocal landscape, the derivative is

$$W'_{n,j}(x) = -\frac{u'_{n,j}(x)}{u_{n,j}(x)^2}.$$

Since  $u_{n,j}(x) = \frac{1}{2}(x - j/n)((j+1)/n - x)$  is a concave quadratic symmetric about  $(2j+1)/(2n)$ , its derivative vanishes uniquely at that midpoint. The second derivative test shows this is a

minimum of  $W_{n,j}$ , because  $u'_{n,j}(x^*) = 0$  and  $u''_{n,j} = -1 < 0$  imply

$$W''_{n,j}(x^*) = -\frac{u''_{n,j}(x^*)}{u_{n,j}(x^*)^2} > 0.$$

Since  $u_{n,j}(x) \rightarrow 0$  at the endpoints of  $\mathcal{I}_{n,j}$ , the reciprocal diverges there, so the midpoint minimum is global. The coincidence of the minimizer of  $W_{n,j}$  and the extremum of  $\psi_n$  follows immediately.  $\square$

**Corollary 1.** *On each nodal interval  $\mathcal{I}_{n,j}$ , the maximum of  $|\psi_n|$  occurs exactly where the reciprocal landscape  $1/u_{n,j}$  is minimized. Thus wave amplitude concentrates at the point where the geometric potential is lowest.*

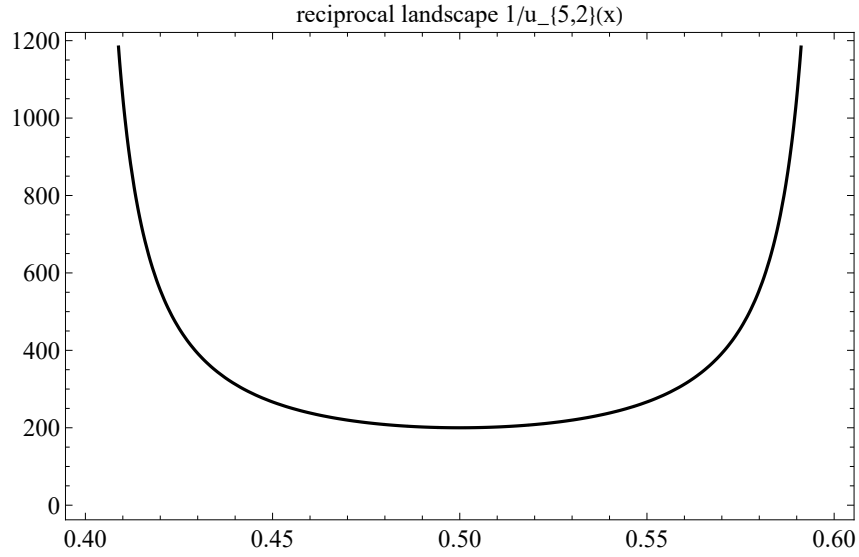


FIGURE 5. Reciprocal landscape  $1/u_{n,j}(x)$  on the interval  $[2/5, 3/5]$  for  $n = 5$ . The unique minimum occurs at  $x = 1/2$ , coinciding with the extremum of  $\psi_5$ . The valley of the reciprocal landscape marks the point of maximal wave amplitude.

**4.3. The Holographic Landscape Theorem.** The final result unifies the local and reciprocal perspectives by showing that the global landscape is itself a spectral object. The static deformation  $u(x)$  arises as the uniformly convergent superposition of all odd vibrational modes. This gives a complete spectral characterization of the landscape.

**Theorem 3** (Holographic Landscape Theorem). *The global landscape  $u(x) = \frac{1}{2}x(1-x)$  admits the convergent spectral representation*

$$(18) \quad u(x) = \sum_{\substack{n=1 \\ n \text{ odd}}}^{\infty} \frac{2\sqrt{2}}{(n\pi)^3} \psi_n(x),$$

*and this representation is unique by orthogonality of the Dirichlet eigenfunctions.*

*Proof.* Starting from the spectral expansion of the Green's function,

$$G(x, \xi) = \sum_{n=1}^{\infty} \frac{\psi_n(x)\psi_n(\xi)}{\lambda_n},$$



integrating both sides against the constant forcing  $f(\xi) = 1$  yields

$$u(x) = \int_0^1 G(x, \xi) d\xi = \sum_{n=1}^{\infty} \frac{\psi_n(x)}{\lambda_n} \int_0^1 \psi_n(\xi) d\xi.$$

Uniform convergence of  $G$  justifies the interchange of summation and integration.

Define

$$c_n := \int_0^1 \psi_n(\xi) d\xi.$$

For  $\psi_n(\xi) = \sqrt{2} \sin(n\pi\xi)$ , we have

$$(19) \quad c_n = \sqrt{2} \int_0^1 \sin(n\pi\xi) \xi d\xi = \frac{\sqrt{2}}{n\pi} [-\cos(n\pi\xi)]_0^1$$

$$(20) \quad = \frac{\sqrt{2}}{n\pi} (1 - (-1)^n).$$

For even  $n$ , the integral vanishes by the antisymmetry of sine about  $\xi = 1/2$ . For odd  $n$ , we have  $(-1)^n = -1$ , so  $c_n = 2\sqrt{2}/(n\pi)$ . Thus

$$c_n = \begin{cases} 0 & n \text{ even} \\ \frac{2\sqrt{2}}{n\pi} & n \text{ odd} \end{cases}$$

Substituting into the series with  $\lambda_n = (n\pi)^2$ , only odd terms survive:

$$u(x) = \sum_{n \text{ odd}} \frac{2\sqrt{2}}{n\pi} \cdot \frac{\psi_n(x)}{(n\pi)^2} = \sum_{n \text{ odd}} \frac{2\sqrt{2}}{(n\pi)^3} \psi_n(x). \quad \square$$

which establishes (18). Uniqueness follows from orthogonality of the eigenbasis.

*Remark 2.* The disappearance of even modes reflects the symmetry of the forcing. The constant function is symmetric about  $x = \frac{1}{2}$ , while even eigenfunctions are antisymmetric, giving  $\int_0^1 \psi_n = 0$ . Only odd eigenfunctions couple to the forcing. This parity selection is the spectral fingerprint of the geometry.

**Proposition 1.** *The series (18) converges uniformly and absolutely. The coefficients decay as  $O(n^{-3})$  for odd  $n$ , so the tail satisfies*

$$\sum_{n > N, n \text{ odd}} \frac{1}{n^3} = O(N^{-2}).$$

*This follows from the regularity  $u \in H^2(0, 1)$  and the classical rate of Fourier coefficient decay for functions with bounded second derivative.*

*Remark 3.* Theorem 3 reveals the landscape as a global spectral object. Each eigenmode contributes with weight  $1/\lambda_n$ . Low modes dominate the curvature of the landscape, while higher modes contribute progressively finer corrections. Together with the segmental and reciprocal theorems, this establishes a complete dictionary between static geometry and dynamic spectrum: locally through nodal and amplitude structure, and globally through the holographic superposition of modes.

## 5. NUMERICAL VERIFICATION

**5.1. Numerical verification of convergence.** This section provides numerical evidence for Theorem 3. The landscape  $u(x) = \frac{1}{2}x(1-x)$  is reconstructed from the truncated spectral sum

$$S_N(x) = \sum_{\substack{n \leq N \\ n \text{ odd}}} \frac{2\sqrt{2}}{(n\pi)^3} \psi_n(x)$$

and compared against the analytic profile on a grid of 1001 equispaced points in  $[0, 1]$ .

**5.1.1. Grid convergence.** Table 1 records the maximum absolute error and relative error (normalised by  $u_{\max} = u(1/2) = 1/8$ ) for several truncation levels  $N$ . The data show rapid convergence consistent with the decay rate  $O(n^{-3})$  predicted by the regularity of  $u$ .

TABLE 1. Grid convergence of spectral partial sums  $S_N(x)$ . Maximum absolute and relative errors computed over 1001 grid points.

$N$	$\max  u - S_N $	relative error (%)
5	$6.74 \times 10^{-4}$	0.539
11	$1.71 \times 10^{-4}$	0.137
21	$5.11 \times 10^{-5}$	0.041
31	$2.41 \times 10^{-5}$	0.019

The monotone decay of the error aligns with the analytic tail estimate  $\sum_{n>N} n^{-3} = O(N^{-2})$  and demonstrates that the spectral expansion converges at a rate controlled by the smoothness of  $u$ .

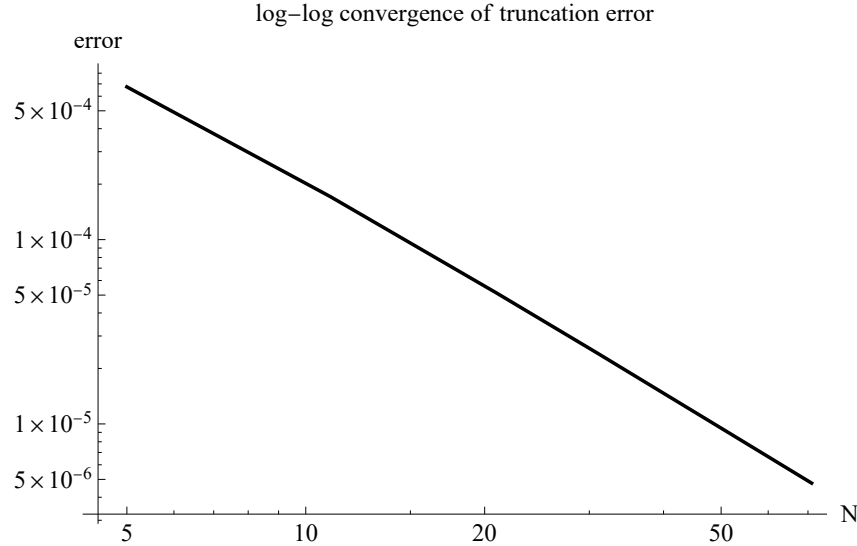


FIGURE 6. Log-log plot of the truncation error  $\max_{x \in [0,1]} |u(x) - S_N(x)|$  versus truncation level  $N$ , illustrating the approximate  $O(N^{-2})$  decay.

5.1.2. *Pointwise accuracy.* To assess uniformity, Table 2 reports the reconstruction error for  $N = 21$  at nine sample locations. The error remains small throughout the domain, with no growth near the boundaries or at the midpoint. This confirms uniform convergence and the absence of Gibbs-type oscillations.

TABLE 2. Pointwise error for  $S_{21}(x)$  at sample locations.

$x$	$u(x)$	$S_{21}(x)$	$ u(x) - S_{21}(x) $
0.1	0.0450	0.044983	$1.68 \times 10^{-5}$
0.2	0.0800	0.079995	$4.69 \times 10^{-6}$
0.3	0.1050	0.105002	$1.59 \times 10^{-6}$
0.4	0.1200	0.120006	$4.92 \times 10^{-6}$
0.5	0.1250	0.125007	$5.98 \times 10^{-6}$
0.6	0.1200	0.120006	$4.92 \times 10^{-6}$
0.7	0.1050	0.105002	$1.59 \times 10^{-6}$
0.8	0.0800	0.079995	$4.69 \times 10^{-6}$
0.9	0.0450	0.044983	$1.68 \times 10^{-5}$

5.1.3. *Visual reconstruction.* Figure 7 overlays the analytic profile with partial sums at three truncation levels. Even the smallest truncation captures the parabolic envelope, and by  $N = 21$  the difference is imperceptible at plotting scale.

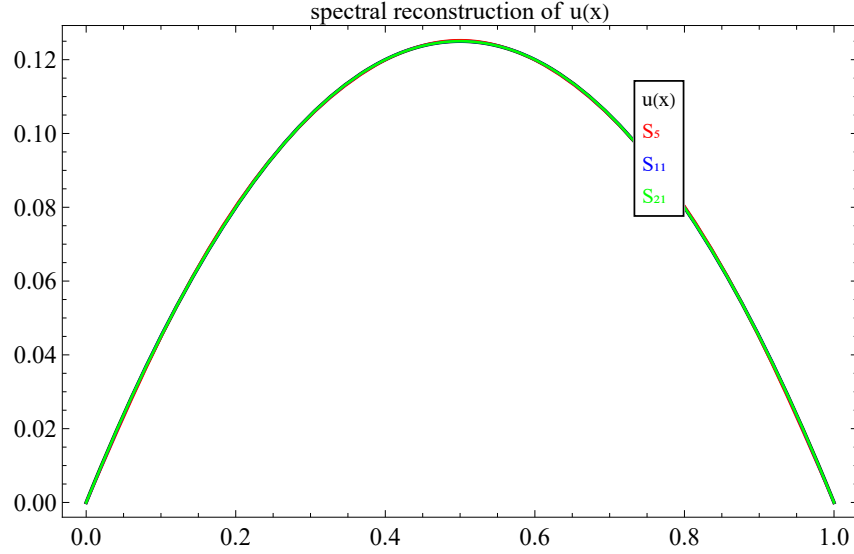


FIGURE 7. Spectral reconstruction of  $u(x)$ . The exact profile  $u(x) = \frac{1}{2}x(1-x)$  (black curve) with partial sums  $S_5$ ,  $S_{11}$ , and  $S_{21}$  (red, blue, green).

The numerical evidence supports the analytic conclusion of Theorem 3. The spectral expansion converges uniformly and at the expected rate  $O(N^{-2})$ , and a modest number of modes is sufficient to reproduce the landscape to near machine precision.

## 6. EXTENSIONS AND RELATED SETTINGS

The correspondences established in one dimension persist, with suitable modifications, in a variety of broader settings. Some of these carry through with full analytic precision, while others serve to illuminate how the landscape framework interacts with additional structure. The following subsections outline these extensions and place the one dimensional results in a wider spectral and geometric context.

**6.1. General forcing.** Consider the Poisson problem with an arbitrary forcing term

$$(21) \quad -u''(x) = f(x), \quad u(0) = u(1) = 0.$$

The Green representation gives

$$u(x) = \int_0^1 G(x, \xi) f(\xi) d\xi = \sum_{n=1}^{\infty} \frac{\psi_n(x)}{\lambda_n} \int_0^1 f(\xi) \psi_n(\xi) d\xi.$$

Writing

$$\hat{f}_n := \int_0^1 f(\xi) \psi_n(\xi) d\xi,$$

the spectral solution becomes

$$(22) \quad u(x) = \sum_{n=1}^{\infty} \frac{\hat{f}_n}{(n\pi)^2} \psi_n(x).$$

When  $f$  is smooth, the coefficients  $\hat{f}_n$  decay rapidly, ensuring uniform convergence. The local landscapes  $u_{n,j}$  generalise by solving

$$-u''_{n,j} = f_{n,j}$$

on each nodal interval, where  $f_{n,j}$  is the average value of  $f$  on that interval. The qualitative behaviour established earlier survives: the segmental structure adapts to the geometry of  $f$ , and the reciprocal principle continues to locate amplitude extrema.

**6.2. Schrödinger operators with potential.** A closely related setting is the one dimensional Schrödinger operator

$$(23) \quad -\psi_n'' + V\psi_n = \lambda_n\psi_n, \quad \psi_n(0) = \psi_n(1) = 0,$$

with a nonnegative potential  $V$ . The landscape now solves

$$-u'' + Vu = 1, \quad u(0) = u(1) = 0.$$

Let  $G_V$  denote the Green kernel of the operator  $-\partial_{xx} + V$ . Its spectral expansion is

$$G_V(x, \xi) = \sum_{n=1}^{\infty} \frac{\psi_n(x) \psi_n(\xi)}{\lambda_n}.$$

Thus,

$$u(x) = \sum_{n=1}^{\infty} \frac{\hat{f}_n}{\lambda_n} \psi_n(x), \quad \hat{f}_n = \int_0^1 \psi_n(\xi) d\xi.$$

The segmental landscape theorem now takes the form

$$-u''_{n,j} + Vu_{n,j} = 1$$

on each nodal interval. The reciprocal landscape again identifies the extrema of the eigenfunctions, although the interaction between the potential and the geometry of the interval produces a richer

pattern of confinement. Potential wells reinforce geometric wells, and the resulting localisation reflects both influences.

**6.3. Alternative boundary conditions.** The landscape framework adapts smoothly to other classical boundary conditions.

**Neumann boundary conditions.** If  $u'(0) = u'(1) = 0$ , the eigenfunctions become

$$\psi_n(x) = \sqrt{2} \cos(n\pi x), \quad n \geq 1,$$

with eigenvalues  $\lambda_n = (n\pi)^2$ . For constant forcing,

$$-u'' = 1$$

gives

$$u(x) = \frac{1}{2} \left( x^2 - x + \frac{1}{6} \right),$$

a symmetric but distinct envelope compared with the Dirichlet case. The local landscape principle is unchanged in structure. The spectral expansion, however, now involves all modes, since the constant forcing has nonzero projection onto both even and odd Neumann eigenfunctions.

**Robin boundary conditions.** For mixed conditions  $\alpha u + \beta u' = 0$  at one or both endpoints, the spectrum remains discrete but is no longer uniformly spaced. The Green representation still yields a spectral expansion for the landscape. Nodal intervals need not have uniform lengths, yet each interval again supports a unique local torsion profile that encodes the geometry of the eigenfunction.

**6.4. Higher dimensions and landscape theory.** In higher dimensions, the landscape is defined by

$$-\Delta u = 1 \quad \text{in } \Omega, \quad u|_{\partial\Omega} = 0,$$

or by  $-\Delta u + Vu = 1$  when a potential is present. The reciprocal  $1/u$  acts as an effective geometric barrier. Exact correspondences, such as the identity between the reciprocal landscape and the location of amplitude extrema, no longer hold in full generality. Nevertheless, several robust principles persist:

- (1) eigenfunctions tend to concentrate where  $1/u$  is small,
- (2) geometric wells of  $u$  interact with potential wells of  $V$ ,
- (3) the Green kernel continues to provide a spectral decomposition of  $u$ .

These observations are central in disordered media, where the landscape provides a geometric predictor of Anderson localisation. The one dimensional model studied in this paper offers an exact and transparent setting in which all these mechanisms can be computed explicitly, clarifying the structure that underlies the more complex theories developed in higher dimensions.

**6.5. Broader implications.** The simplicity of the one dimensional setting exposes analytic mechanisms that are otherwise concealed by geometric complexity. The segmental landscape theorem describes nodal partitioning with complete clarity. The reciprocal principle identifies the precise geometry of amplitude localisation. The holographic landscape theorem reveals the static deformation as a spectral superposition of vibrational modes. Together, these principles form a dictionary that unifies static geometry with dynamic oscillation.

Looking forward, several directions invite further exploration. These include:

- (1) domains with corners or singular potentials,

- (2) discrete analogues on finite graphs or arithmetic settings,
- (3) numerical methods shaped adaptively by the landscape,
- (4) the role of parity and symmetry in holographic expansions.

The central insight remains that the geometry of the landscape encodes the full spectral content of the operator. The vibrational modes shape the static deformation, and the static deformation in turn predicts the behaviour of the vibrational modes. The sagging string contains, within its equilibrium profile, the sum of all its possible sounds.

*Mathematica code.* All computational notebooks and scripts used to generate the numerical figures in this paper are available from the author upon request.

## REFERENCES

- [1] M. Kac, *Can one hear the shape of a drum?* American Mathematical Monthly **73** (1966), 1–23.
- [2] M. Filoche and S. Mayboroda, *Universal mechanism for Anderson and weak localization* Proceedings of the National Academy of Sciences **109** (2012), 14761–14766.
- [3] M. Filoche and S. Mayboroda, *The landscape of Anderson localization in a disordered medium* Contemporary Mathematics **601** (2013), 113–121.
- [4] R. Courant and D. Hilbert, *Methods of Mathematical Physics, Vol. I* Wiley Interscience, 1953.
- [5] S. R. Jain and R. Samajdar, *Nodal portraits of quantum billiards: domains, statistics, and complexity* Reviews of Modern Physics **89** (2017), 045005.
- [6] A. Zettl, *Sturm–Liouville Theory* American Mathematical Society, 2005.
- [7] G. Teschl, *Mathematical Methods in Quantum Mechanics* American Mathematical Society, 2014.
- [8] L. C. Evans, *Partial Differential Equations* American Mathematical Society, 1998.
- [9] D. Gilbarg and N. S. Trudinger, *Elliptic Partial Differential Equations of Second Order* Springer, 2001.
- [10] C. Bandle, *Isoperimetric Inequalities and Applications* Pitman, 1992.
- [11] I. Chavel, *Eigenvalues in Riemannian Geometry* Academic Press, 1984.
- [12] R. Courant, *Ein allgemeiner Satz zur Theorie der Eigenschwingungen* Nachrichten der Königlichen Gesellschaft der Wissenschaften zu Göttingen (1923).
- [13] P. W. Anderson, *Absence of diffusion in certain random lattices* Physical Review **109** (1958), 1492–1505.
- [14] J. B. Keller, *Lower bounds and isoperimetric inequalities for eigenvalues* Journal of Mathematical Physics **2** (1961), 262–266.

Email address: `aryaman.chandra@gmail.com`

Email address: `sudhirranjan@somaiya.edu`